Evolution of the 2012 July 12 CME from the Sun to the Earth: Data-Constrained Three-Dimensional MHD Simulations

F. Shen[1], C. Shen[2], J. Zhang[3], P. Hess[3], Y. Wang[2] and X. Feng[1]

[1]State Key Laboratory of Space Weather, NSSC, CAS, China

[2]School of Earth and Space Sciences, USTC, China

[3]School of Physics, Astronomy and Computational Sciences, George Mason University, USA

F. Shen, C. Shen, J. Zhang et al., *JGR*, 2014

2015-03-03, AOSWA-3, Fukuoka, Japan

SIGMA
WEATHER GROUP

Outline:

- Introduction to the 2012 July 12-16 CME event
- 3D MHD Model and Simulation Method
- Kinematic Evolution of the CME
- Conclusions

SIGMA
WEATHER GROUP

The Time Line of the Event

[Hess and Zhang, APJ, 2014]

• 07/12 16:48 UT: CME first appear in SOHO/C2	0 hr
• 07/12 18:54 UT: CME at 20 Rs	2 hr 06 min
• 07/13 00:49 UT: CME at 50 Rs	8hr 01 min
• 07/13 06:49 UT: CME at 80 Rs	14 hr 01 min
• 07/14 17:00 UT: Shock arrival at 1 AU	48 hr 12 min
• 07/15 06:00 UT: Magnetic Cloud arrival at 1 AU	61 hr 12 min
• 07/15 19:00 UT: Peak time of Dst (-127 nT)	74 hr 12 min
• 07/17 14:00 UT: Magnetic Cloud end at 1 AU	117 hr 12 min

SIGMA WEATHER GROUP

Coronagraph **Observations**

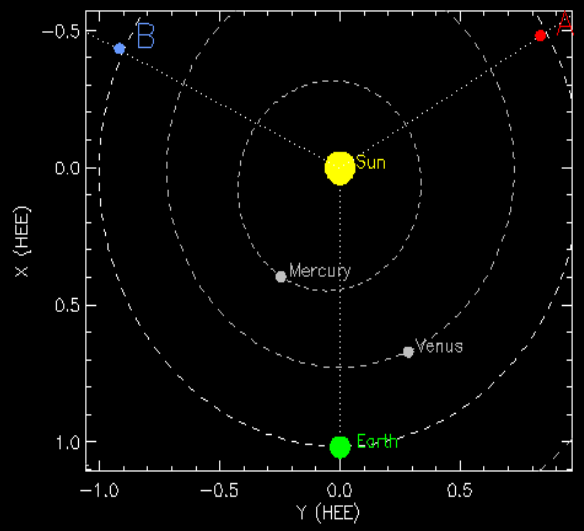

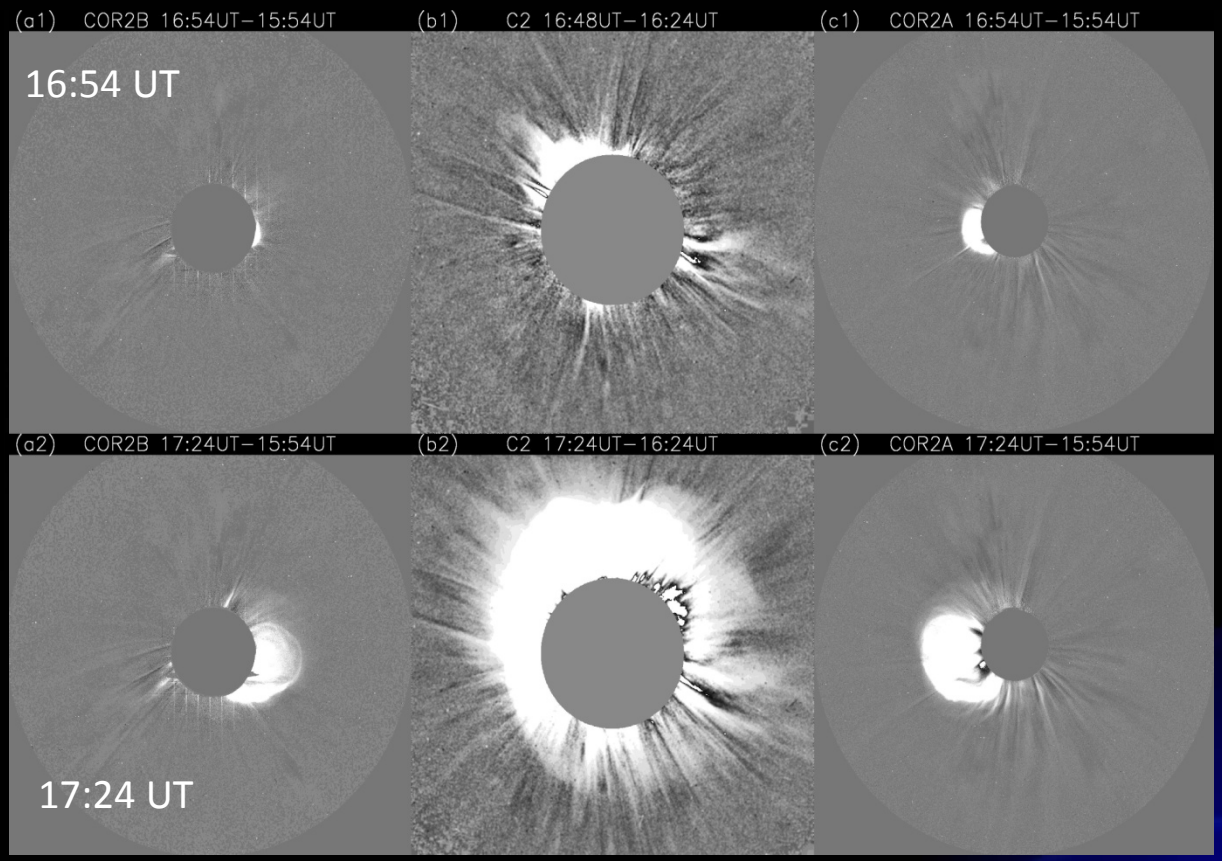

STEREO-A COR2 SOHO/LASCO C2 STEREO-B COR2

The event was recently studied by several authors using observational or theoretical method

[Möstl et al., 2014; Cheng et al., 2014; Dudík et al., 2014; Hess and Zhang, 2014]

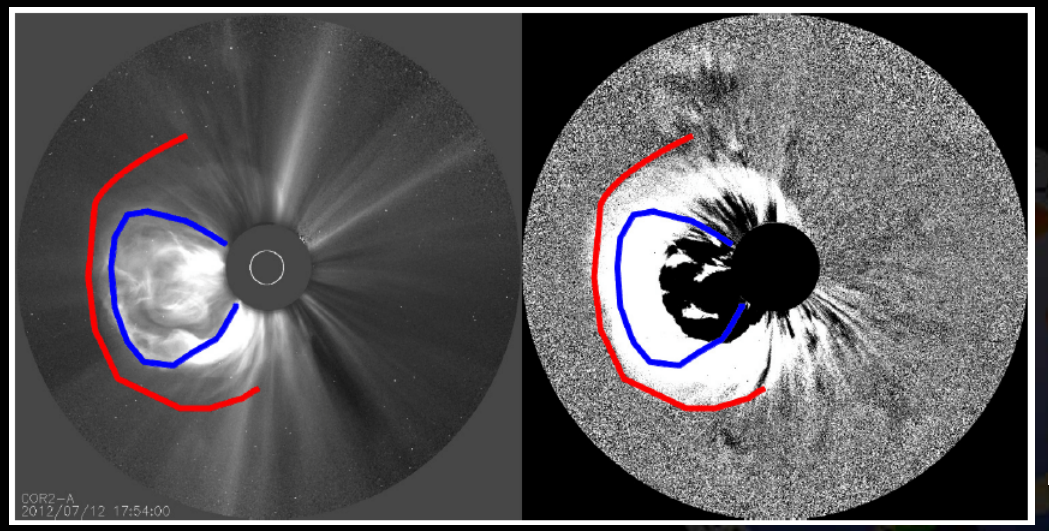

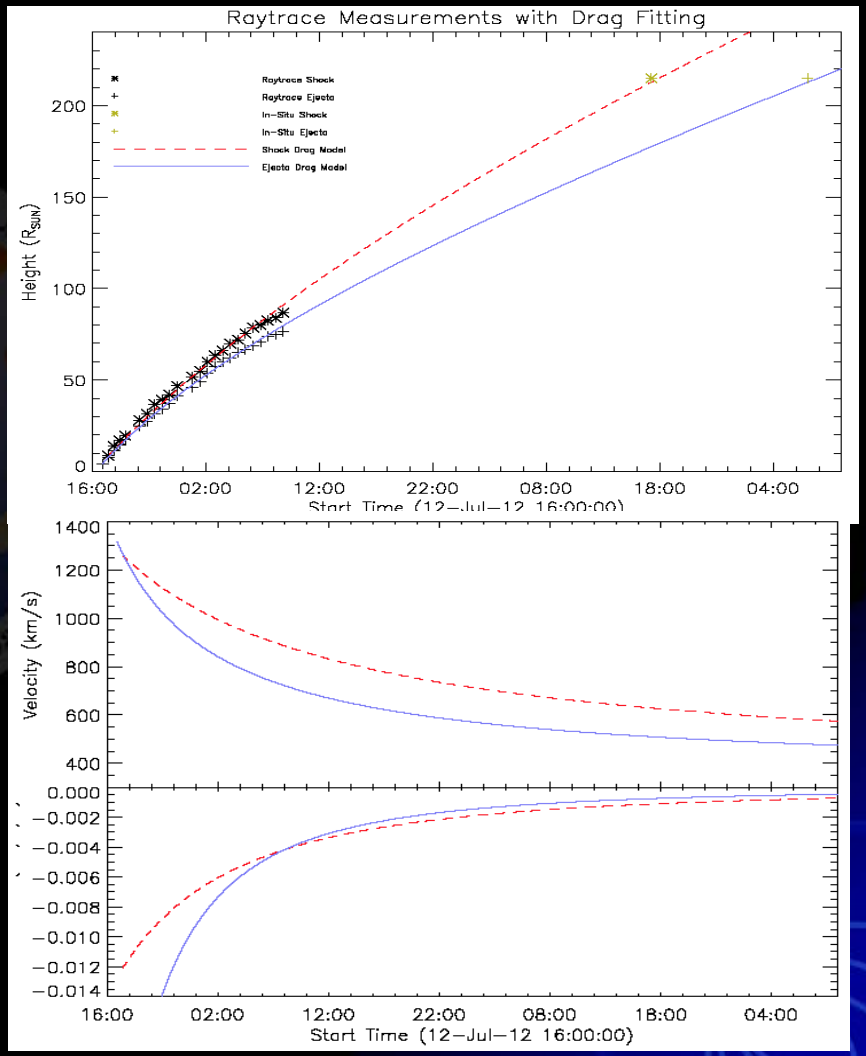

- Drag model: shock front
- Drag model: ejecta front

[Hess and Zhang, 2014]

[Möstl et al., 2014, APJ]

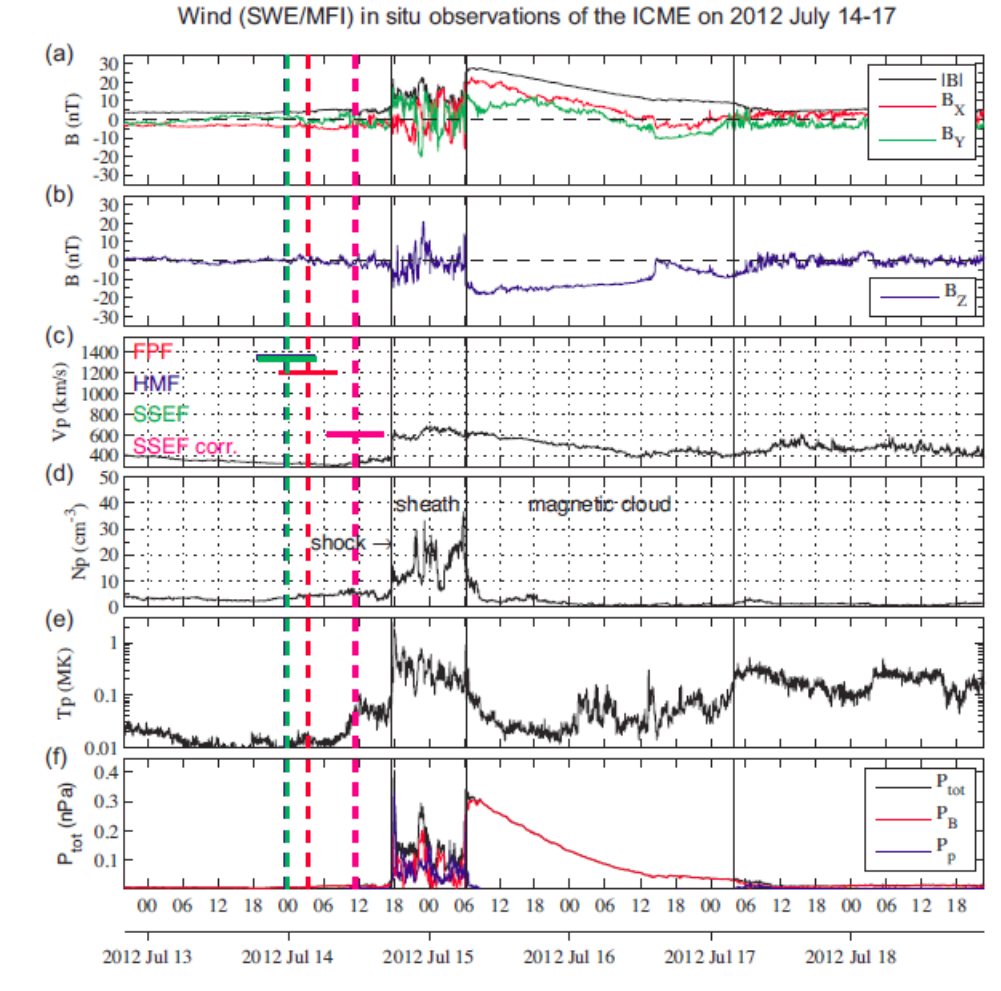

FIG. 3.— In situ solar wind observations from the near-Earth Wind spacecraft, at the Sun-Earth L1 point, between 2012 July 13–18. From top to bottom: (a) Total magnetic field strength and B_X and B_Y components (*in Geocentric Solar Ecliptic* or GSE coordinates). (b) Magnetic field component B_Z in GSE. (c) Proton bulk speed. (d) Proton number density. (e) Proton temperature. (f) Magnetic (P_B), plasma (P_p) and total pressure (P_{tot}). Predicted arrival times from the FPF (red), HMF (blue) and SSEF (green) models are indicated as vertical dashed lines. The speeds predicted by the same models are shown in panel (c) as horizontal bars, in similar colors, for direct comparison to the in situ proton bulk speed. The width of the horizontal bars corresponds to the estimated error in arrival time resulting from the manual selection of points (±10% of the total CME transit time). The corrected arrival time (in version 1, see text) and the corrected speed ("SSEF corr.") from section 3.2 are shown as pink vertical and horizontal lines, respectively.

3D MHD Model and Simulation Method

[Feng et al., 2003; 2005; Shen et al., 2007; 2011; 2012; 2013]

Computational domain for 3D MHD

- **Sun-centered spherical coordinate system (r, θ, φ)**
- **r-axis in the ecliptic plane**
- **Earth (L1 point) located at r = 215 Rs (213 Rs), $\theta = 0^\circ$, and $\varphi = 180^\circ$**
- **The computational domain: 1 Rs $\leq r \leq$ 220 Rs; $-89^\circ \leq \theta \leq 89^\circ$ and $0^\circ \leq \varphi \leq 360^\circ$.**

- 3D time-dependant MHD equations:

$$\frac{\partial U}{\partial t}+\frac{1}{r^2}\frac{\partial r^2 F}{\partial r}+\frac{1}{r\sin\theta}\frac{\partial \sin\theta G}{\partial \theta}+\frac{1}{r\sin\theta}\frac{\partial H}{\partial \varphi}=S$$

where

$$U=\begin{pmatrix}\rho\\ \rho u_r\\ \rho u_\theta\\ \rho v_\varphi\\ B_r\\ B_\theta\\ B_\varphi\\ p\end{pmatrix},\quad F=\begin{pmatrix}\rho u_r\\ \rho u_r^{\,2}\\ \rho u_r u_\theta\\ \rho u_r v_\varphi\\ 0\\ u_r B_\theta-u_\theta B_r\\ u_r B_\varphi-v_\varphi B_r\\ p u_r\end{pmatrix},\quad G=\begin{pmatrix}\rho u_\theta\\ \rho u_r u_\theta\\ \rho u_\theta^{\,2}\\ \rho u_\theta v_\varphi\\ u_\theta B_r-u_r B_\theta\\ 0\\ u_\theta B_\varphi-v_\varphi B_\theta\\ p u_\theta\end{pmatrix},\quad H=\begin{pmatrix}\rho v_\varphi\\ \rho u_r v_\varphi\\ \rho u_\theta v_\varphi\\ \rho v_\varphi^{\,2}\\ v_\varphi B_r-u_r B_\varphi\\ v_\varphi B_\theta-u_\theta B_\varphi\\ 0\\ p v_\varphi\end{pmatrix}$$

$$
S = \begin{pmatrix}
0 \\
-\frac{1}{r^2}\frac{\partial}{\partial r}\left(r^2\left(p+\frac{B^2}{2\mu_0}-\frac{B_r{}^2}{\mu_0}\right)\right)+\frac{1}{r\sin\theta}\frac{\partial}{\partial\theta}\left(\frac{\sin\theta B_r B_\theta}{\mu_0}\right)+\frac{1}{r\sin\theta}\frac{\partial}{\partial\varphi}\left(\frac{B_r B_\varphi}{\mu_0}\right) \\
\quad +\frac{2p}{r}+\rho\frac{u_\theta{}^2+v_\varphi{}^2}{r}+\frac{B_r{}^2}{r\mu_0}-\frac{\rho GM_s}{r^2}+f_r \\
\frac{1}{r^2}\frac{\partial}{\partial r}\left(\frac{r^2 B_r B_\theta}{\mu_0}\right)-\frac{1}{r\sin\theta}\frac{\partial}{\partial\theta}\left(\sin\theta\left(p+\frac{B^2}{2\mu_0}-\frac{B_\theta{}^2}{\mu_0}\right)\right)+\frac{1}{r\sin\theta}\frac{\partial}{\partial\varphi}\left(\frac{B_\theta B_\varphi}{\mu_0}\right) \\
\quad +\frac{\cot\theta}{r}\left(p+\frac{B^2}{2\mu_0}\right)+\rho\frac{v_\varphi{}^2\cot\theta-u_r v_\theta}{r}-\frac{B_\varphi{}^2\cot\theta-B_r B_\theta}{r\mu_0}+f_\theta \\
\frac{1}{r^2}\frac{\partial}{\partial r}\left(\frac{r^2 B_r B_\varphi}{\mu_0}\right)+\frac{1}{r\sin\theta}\frac{\partial}{\partial\theta}\left(\frac{\sin\theta B_\varphi B_\theta}{\mu_0}\right)-\frac{1}{r\sin\theta}\frac{\partial}{\partial\varphi}\left(\sin\theta\left(p+\frac{B^2}{2\mu_0}-\frac{B_\varphi{}^2}{\mu_0}\right)\right) \\
\quad -\rho\frac{u_r v_\varphi+u_\theta v_\varphi\cot\theta}{r}+\frac{B_r B_\varphi+B_\theta B_\varphi\cot\theta}{r\mu_0}+f_\varphi \\
0 \\
(B_\theta u_r-B_r u_\theta)/r \\
(u_\theta B_\varphi-v_\varphi B_\theta)\cot\theta+(v_r B_\varphi-v_\varphi B_r)/r \\
-(\gamma-1)p\nabla\bullet\vec{v}+(\gamma-1)Q
\end{pmatrix}
$$

Inertial centrifugal forces

volumetric heating function

3D MHD Model and Simulation Method

[Feng et al., 2003; 2005; Shen et al., 2007; 2011; 2012; 2013]

- **Modified Lax-Friedrichs MHD COrona-INterplanetary Coupling Model: COIN TVD-MHD Model**

Method description

I) Use different numerical method to deal with corona area and interplanetary area

II) Non-reflecting Boundary Conditions at inner boundary

III) Parallel Implementation with Fortran **MPI**

IV) The numerical 3D MHD scheme used was a modified total variation diminishing /Lax-Friedrichs (TVD/LF) type scheme with **consideration of divergence-free condition**

V) The potential field, extrapolated from the observed line-of-sight magnetic field of CR2125 on the photosphere, is used as the initial magnetic field.

- Distribution of background solar wind in Carrington Rotation (CR)2125

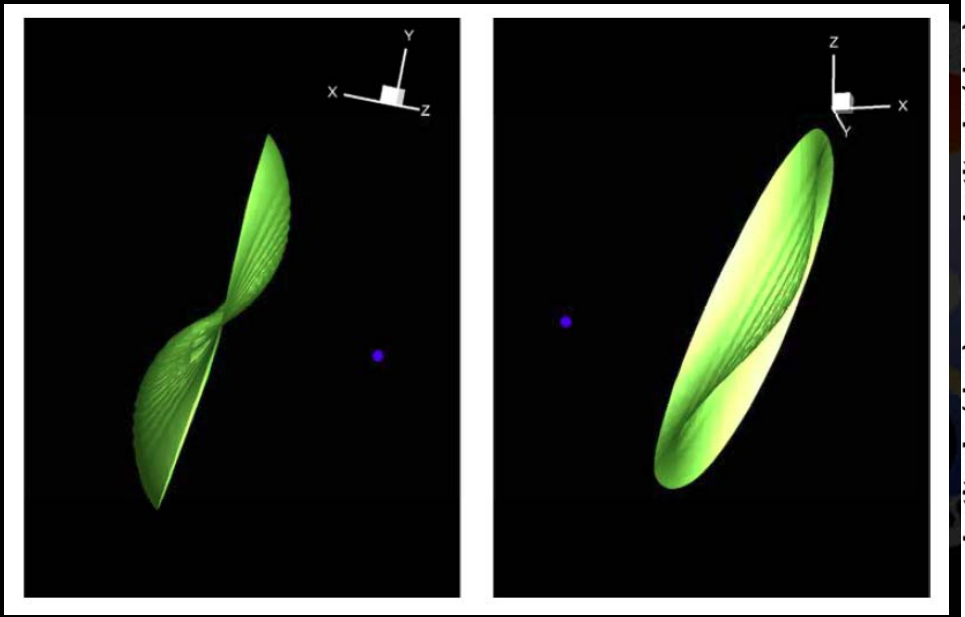

Figure 1. The calculated steady-state 3D shape of the steady current sheet distribution, from 1 R_s to 220 R_s at 100 hours

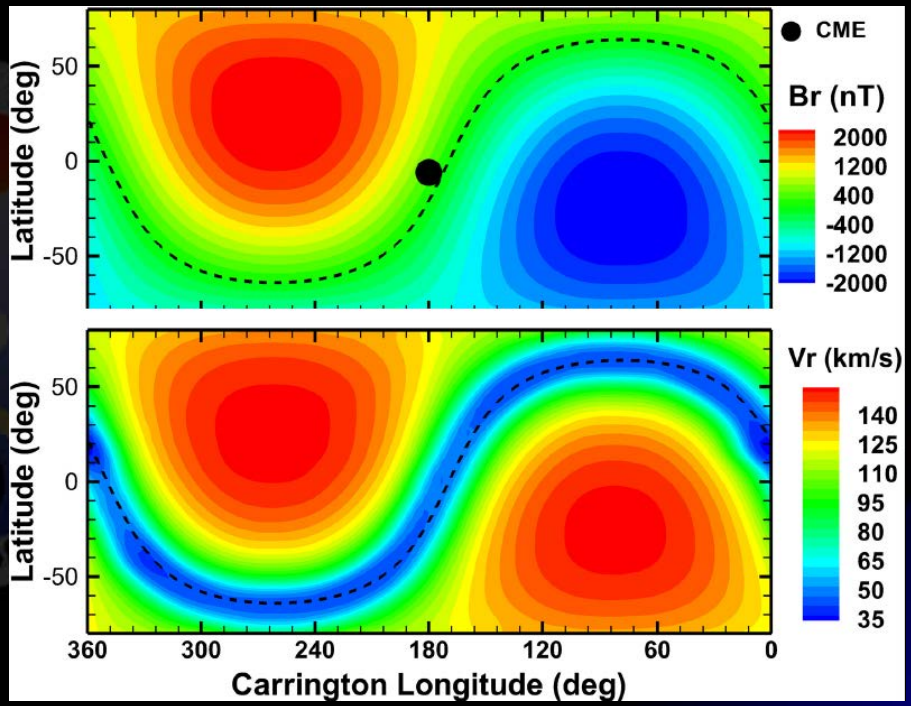

Figure 2. The steady-state distribution of radial-component of magnetic field (top) and velocity (bottom) at 5 Rs

CME Model

——Magnetized Plasma Blob Model :

[Shen et al., JGR, 2011a; 2011b; 2012]

(1) A high-density, -velocity, -temperature, and magnetized plasma blob is superposed on the background solar wind model;

(2) The density, radial velocity and temperature profile of the initial perturbation are defined as follows:

$$\begin{cases} \rho_{CME}(r,\theta,\varphi) = \dfrac{\rho_{\max}}{2}\left(1-\cos\left(\pi\dfrac{a_{cme}-a(r,\theta,\varphi)}{a_{cme}}\right)\right) \\ V_{CME}(r,\theta,\varphi) = \dfrac{v_{\max}}{2}\left(1-\cos\left(\pi\dfrac{a_{cme}-a(r,\theta,\varphi)}{a_{cme}}\right)\right) \\ T_{CME}(r,\theta,\varphi) = \dfrac{T_{\max}}{2}\left(1-\cos\left(\pi\dfrac{a_{cme}-a(r,\theta,\varphi)}{a_{cme}}\right)\right) \end{cases}$$

(3) The initial magnetic field is defined as

$$\begin{cases} B_{r_{CME}}(r,\theta,\varphi) = -\dfrac{1}{r^2 \sin\theta}\dfrac{\partial \psi(r,\theta,\varphi)}{\partial \theta} \\ B_{\theta_{CME}}(r,\theta,\varphi) = \dfrac{1}{r \sin\theta}\dfrac{\partial \psi(r,\theta,\varphi)}{\partial r} \end{cases}$$

where

$$\psi(r,\theta,\varphi) = \psi_0 (a(r,\theta,\varphi) - \frac{a_{CME}}{2\pi}\sin(\frac{2\pi a(r,\theta,\varphi)}{a_{CME}}))$$

is the magnetic flux function

(4) This initial perturbation will be given by the following relation:

$$\begin{cases} \rho = \rho_0 + \rho_{CME}(r,\theta,\varphi) \\ v_r = v_{r0} + V_{CME}(r,\theta,\varphi) \\ T = T_0 + T_{CME}(r,\theta,\varphi) \\ B_r = B_{r0} + B_{rCME}(r,\theta,\varphi) \\ B_\theta = B_{\theta 0} + B_{\theta CME}(r,\theta,\varphi) \end{cases}$$

Initialization for 2012July12 Event from observational data

[Hess and Zhang, APJ, 2014]

◎ The propagation direction of the CME is S09W01 deduced by using STEREO observations and Graduated Cylindrical Shell (GCS) model;

◎ The centre of the initial plasma blob is at latitude θ_{cme}=-9^{o}, and longitude φ_{cme}=179^{o};

◎ First STEREO/COR A Appearance date Time: July 12, 1654UT, CME arrival time at L1 point: July 14, 1700UT, Shock transit time: ~48hrs;

◎ Initial speed of CME at 5 Rs is ~1494 km/s.

Kinematic Evolution of the CME

- Comparisons with Coronagraph Observations

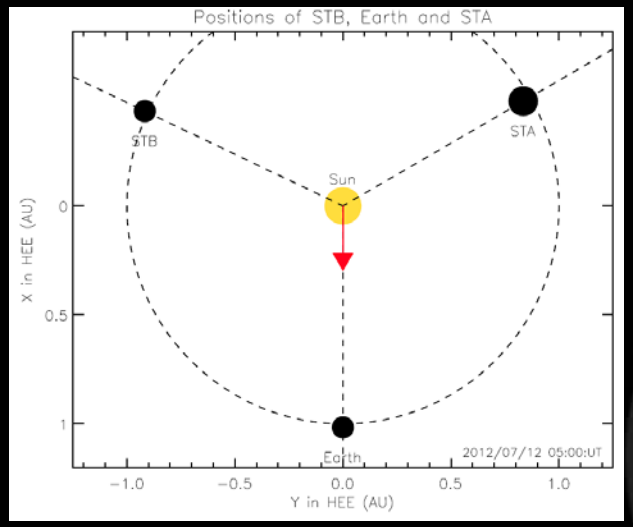

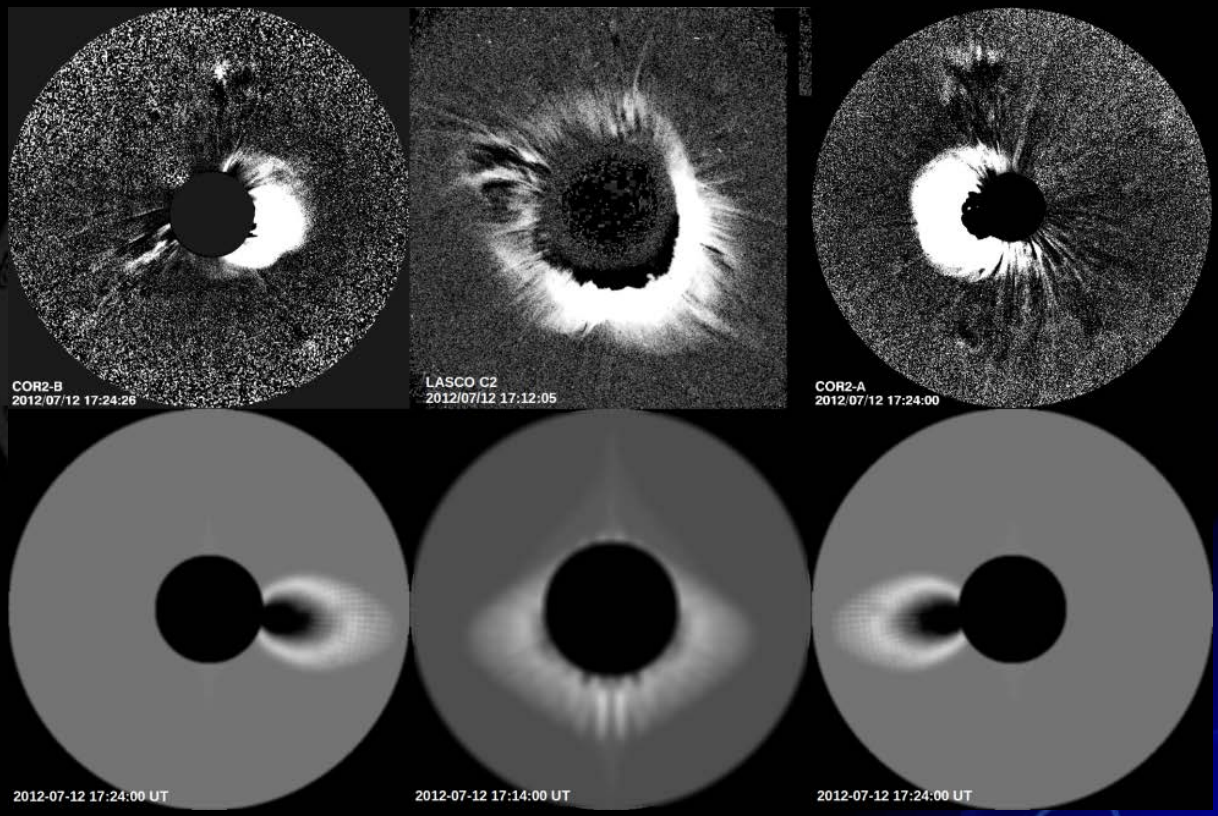

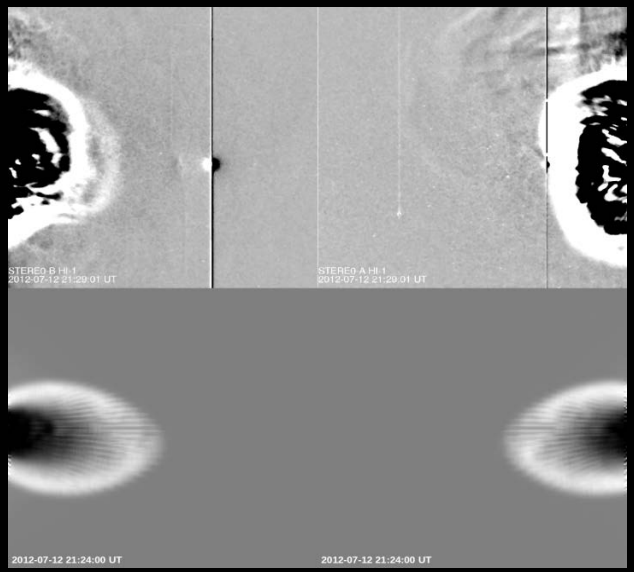

SIGMA
WEATHER GROUP

- Synthetic LASCO/C2/C3, STEREO/COR2A/COR2B movies, showing white brightness from simulated density result:

C2

COR2A

COR2B

C3

STB SOHO STA

Comparisons with Time-Elongation Maps (J-maps)

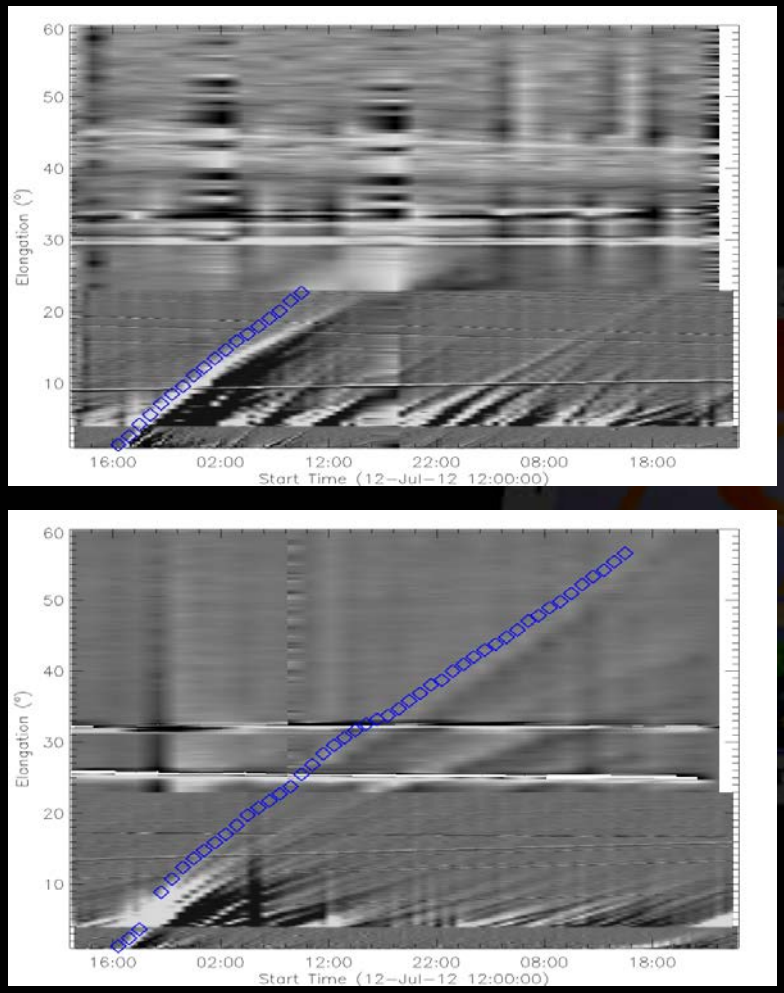

Figure 3. Real J-maps constructed based on the imaging data from COR2, HI1 and HI2 imagers onboard STA and STB

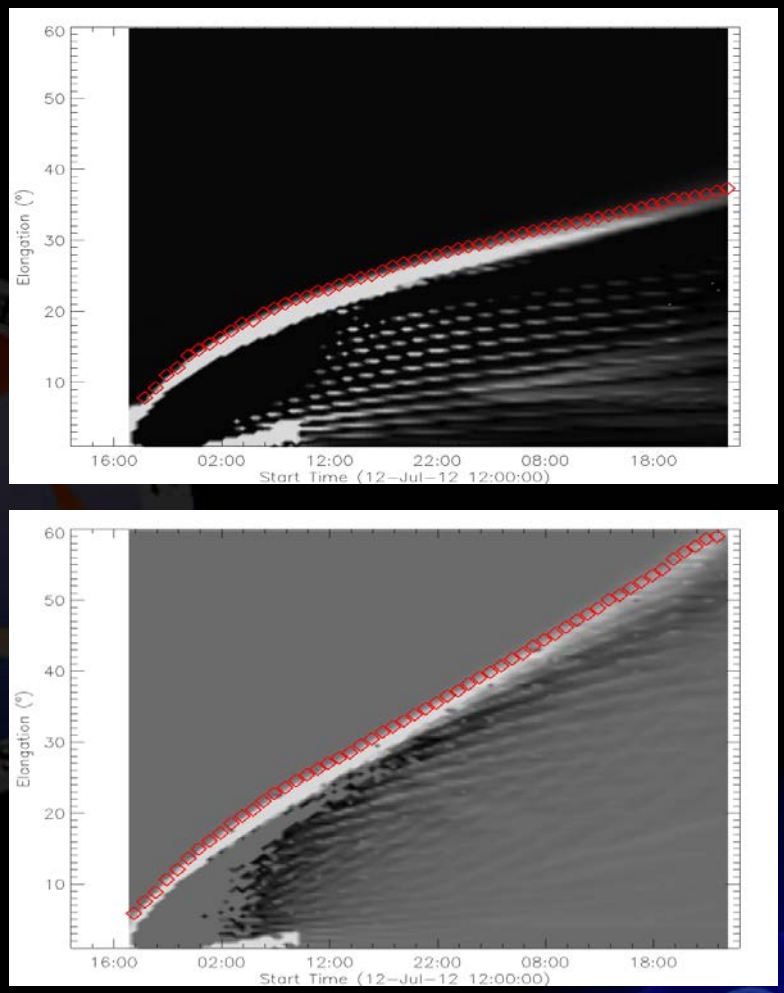

Figure 4. Synthetic J-maps corresponding to the position of STA and STB

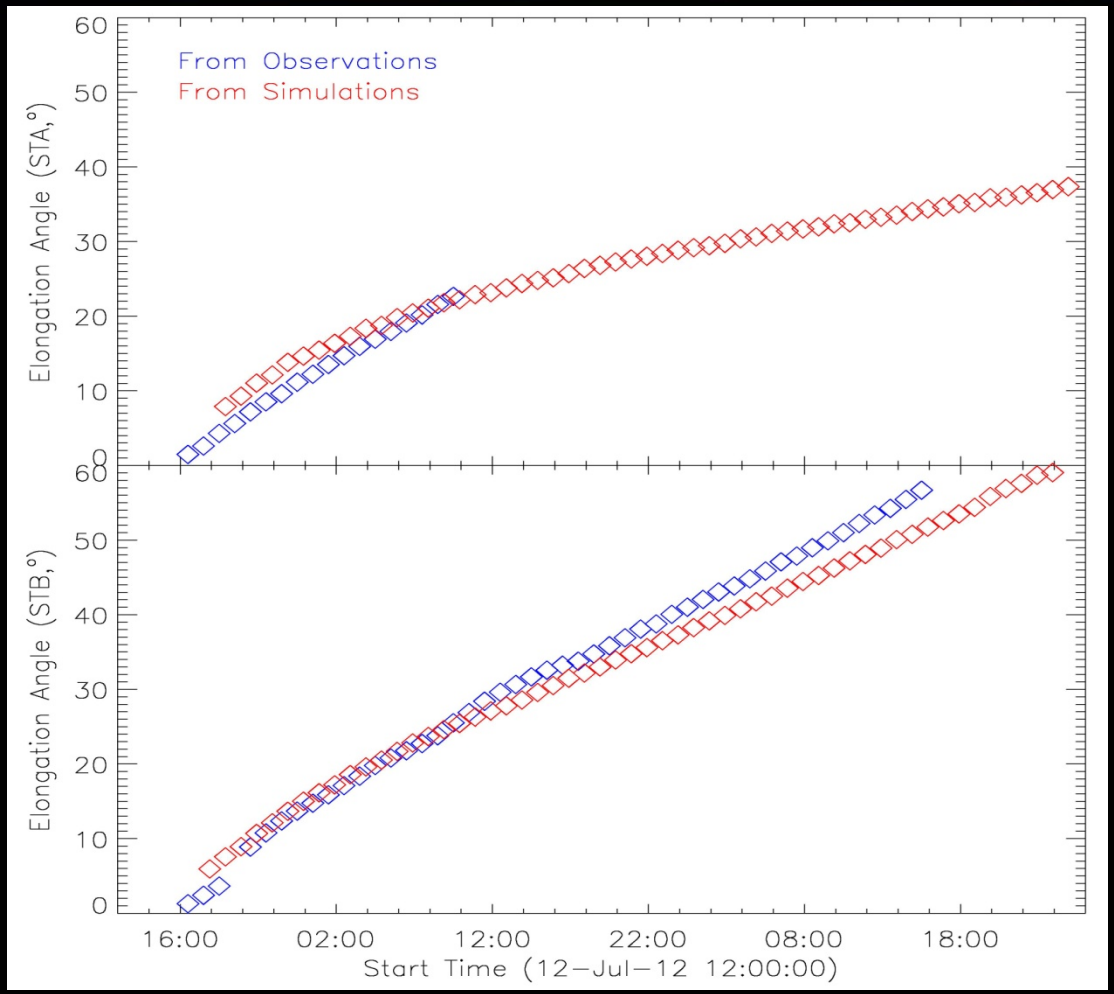

Figure 5. Comparison between time-elongation profiles from the observations and the synthetic images derived from simulation corresponding to the position of STA (top) and STB (bottom).

SIGMA WEATHER GROUP

3D Kinetic Evolution of the CME

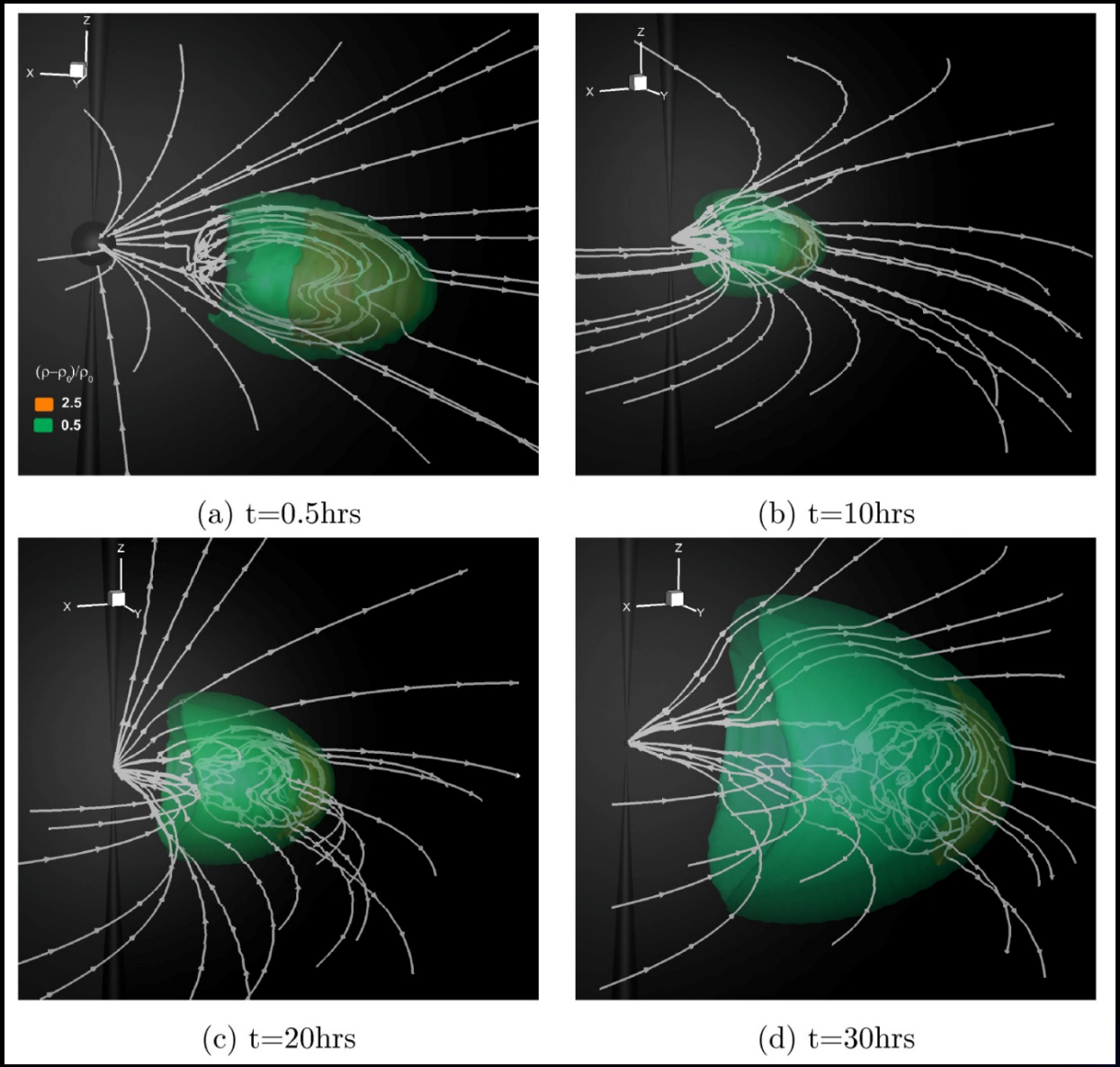

Figure 6. 3-D view of the relative density $(\rho - \rho_0)/\rho_0$ distribution

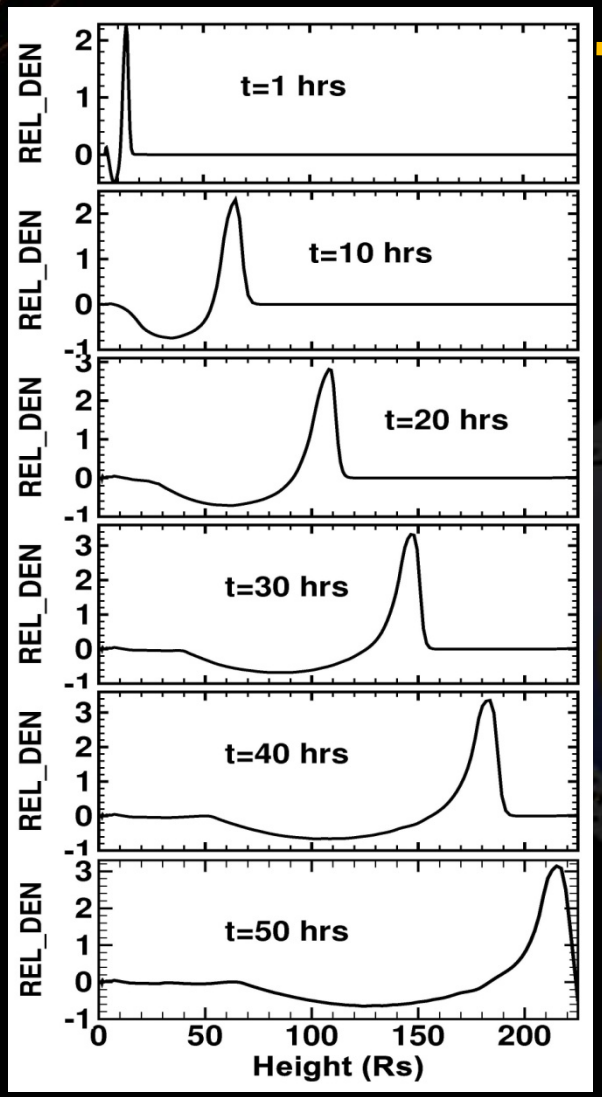

Figure 7. Evolution of the relative density along the Sun-Earth line.

Supposing the shock locating at the position with the maximum of the density gradient

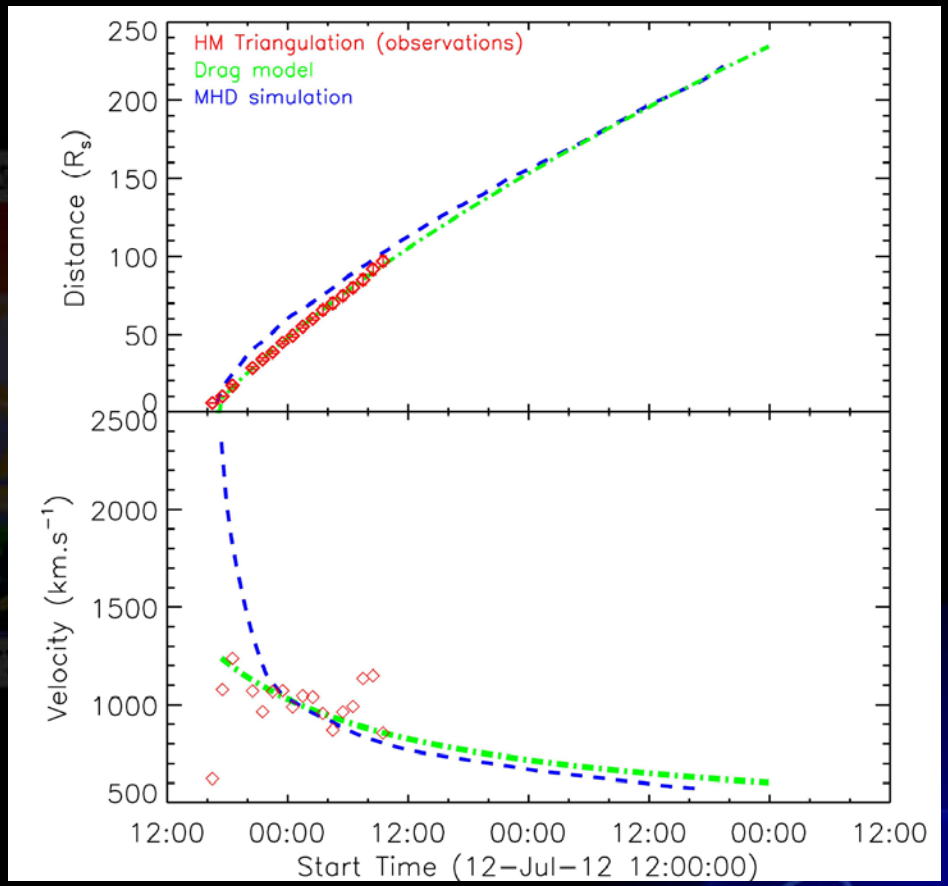

Figure 8. Time-height plot and the time-speed plot of the shock

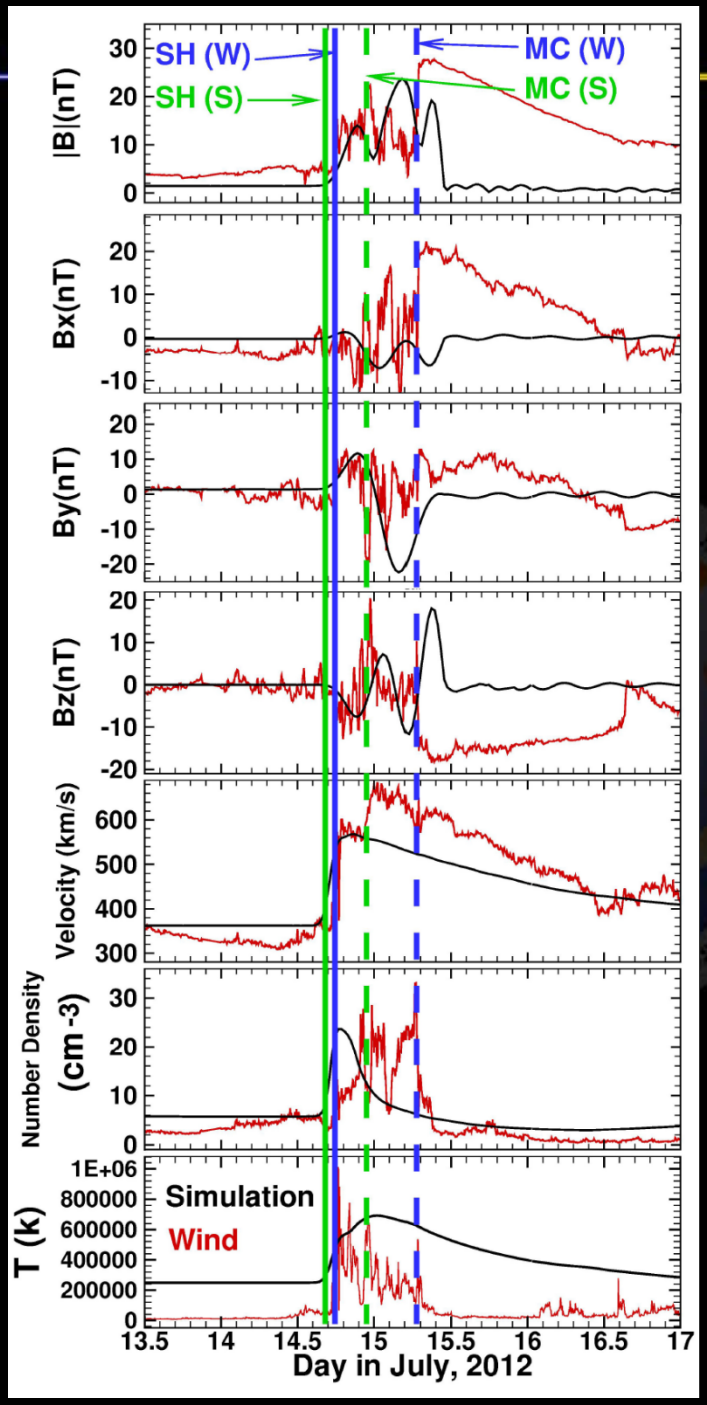

Figure 9. A comparison of the MHD simulation of the magnetic field and plasma parameters using the measured (Wind spacecraft) magnetic field and solar wind parameters at 1 AU.

Conclusions

- We have investigated the evolution of the CME in a realistic ambient solar wind for the July 12-16, 2012 event by using the 3D data-constrained COIN-TVD MHD simulation;
- From the comparisons with remote sensing observations and J-maps ,we are able to reproduce successfully the observations in STA and STB field-of-view, for both the CME morphology and the CME kinematics;
- When the CME evolves to ICME reaching 1 AU, its physical parameters resemble the observations of the ICME recorded by the Wind spacecraft: the transit time of the shock is approximately reproduced; the velocity, the total magnetic field, the temperature and the density peak value is very close to the realistic values during the peak period.
- Our next goal is to apply this 3D MHD model to space weather prediction based on the observational data.

Thanks